Design of High Current Nanosecond Resonant Pulse Drivers for Laser Diodes, Lidar, and other Applications

EPC
EFFICIENT POWER CONVERSION

John S. Glaser, Director of Applications Engineering; Efficient Power Conversion Corporation

1.0 Abstract

Gallium nitride (GaN) power FETs and ICs have found broad application in nanosecond high current pulse generators. One application in particular, time-of-flight (ToF) lidar, has been enabled by cost-effective GaN-based diode laser drivers capable of generating current pulses with pulse widths of a few nanoseconds and peak currents of tens to hundreds of amps. EPC has been at the forefront of this and other applications that benefit from the extreme speed, repetitive peak current capability, low inductance and high reliability inherent to GaN power semiconductor technology. EPC supports a wide range of current pulse capability, and makes available a series of development boards so that engineers needing or wanting this capability can get up to speed quickly. The schematics, bills of material, and PCB layout files for these designs are freely available for download. High current pulse drivers are conceptually simple, but they are dominated by parasitics, especially inductance, and this presents many challenges. This article attempts to provide the basic background and design methods that are used to achieve repeatable and predictable single digit nanosecond high current pulses.

2.0 Introduction

Gallium nitride (GaN) power FETs and ICs have demonstrated order-of-magnitude improvements in performance figures-of-merit over silicon MOSFETs while achieving cost parity to silicon on an equal voltage and $R_{DS(on)}$ basis [1]. The key improvements are increased switching speed and decreased size, and the obvious application is switched-mode power conversion. Hence, the rapidly increasing adoption of GaN in power converters is not surprising, especially for those uses needing superior efficiency, power density, and reliability. Less predictable is the enabling of new applications that previously simply didn't exist, were impractical, or astronomically expensive. One recent example is the development of cost-effective time-of-flight (ToF) lidar-based three-dimensional imaging, which is finding widespread use in autonomous navigation for many applications including automotive ADAS systems and robots [2], [3], [4], [5]. GaN power devices

have made possible the development and commercialization of cost-effective lidar systems because they enable tiny laser diode drivers capable of pulses of 10s to 100s of amps in a few short nanoseconds. What does tiny mean? As a point of reference, one of the designs in this article uses a 2 x 3.5 x 0.64 mm chip-scale GaN FET to drive lasers with pulses in excess of 200 A at tens or hundreds of kilohertz for years, i.e. many trillions of pulses with no signs of degradation [6]. All this can be accomplished with standard PCBs and at low cost with few components.

While this article will focus on laser diode drivers for lidar applications, the design methods are suitable for any application where high current nanosecond pulses are needed. It is safe to say that this a wide open space, because the capability is new. Diode laser machining, high-power impulse radar, and medical imaging might be possibilities, and the reader is invited to use their imagination. What can you do with tens or hundreds of amps in a few nanoseconds?

This article will cover the following topics: First, there will be short discussion of lidar, laser diodes, and pulse requirements. This will be followed by a review of GaN power semiconductor technology with an eye towards pulse power applications. Next will be an introduction to resonant pulse laser drivers, followed by a detailed discussion of resonant pulse circuit design and a design procedure. This will be followed by a design example based on EPCs EPC9179 laser driver [7]. The next section will present experimental results of EPC's laser drivers. The last technical section will cover a broad array of ancillary topics including alternate driver topologies, voltage and current sensing, and resonant capacitor charging, as well as potential design pitfalls. Finally, the Appendix summarizes currently active EPC demonstration boards targeted at lidar and other high current nanosecond pulse applications.

3.0 Lidar and the need for high power laser transmitters

Lidar is a form of radar where the electro-magnetic radiation happens to be in the optical band [8]. A typical lidar system is shown in Figure 1. In the last few years, one particular form of lidar, time-of-flight (ToF) distance measurement, has become commercially produced in high volume. If a laser is used as the optical source, one can measure the distance of a small spot even at long range. When combined with steerable optics, one can sweep the spot distance measurement and map objects in 3D space.

There are two main kinds of ToF lidar: direct time-of-flight (DToF) and indirect time-of-flight (IToF). We will look only at DToF lidar requirements in this article. The basic operating principle is shown in Figure 2. In DToF systems, single pulses are transmitted, reflected from a target and detected. The time between the transmitted and detected pulses, i.e. the time of flight, is measured and the distance can be calculated from Equation 1:

(1)

$$t_d = 2d/c$$

Please keep in mind that this is a very simplified view, but the basic principle is valid.

4.0 DToF lidar transmitter requirements

DToF lidar requires short duration, high power optical pulses of a specified wavelength, and these requirements usually come to the transmitter designer from the lidar system design level. System level concerns are typically range, field of view, pixel count, frame rate, and operating environment. The latter may include sources of interference (the sun, other lidars, multipath) and signal attenuation (rain, fog, haze, dirty optics), as well as regulatory concerns (eye safety). The designer needs numerical targets for desired wavelength, pulse duration, and pulse power. This section will provide a brief overview of typical requirements for cost-effective DToF lidar systems.
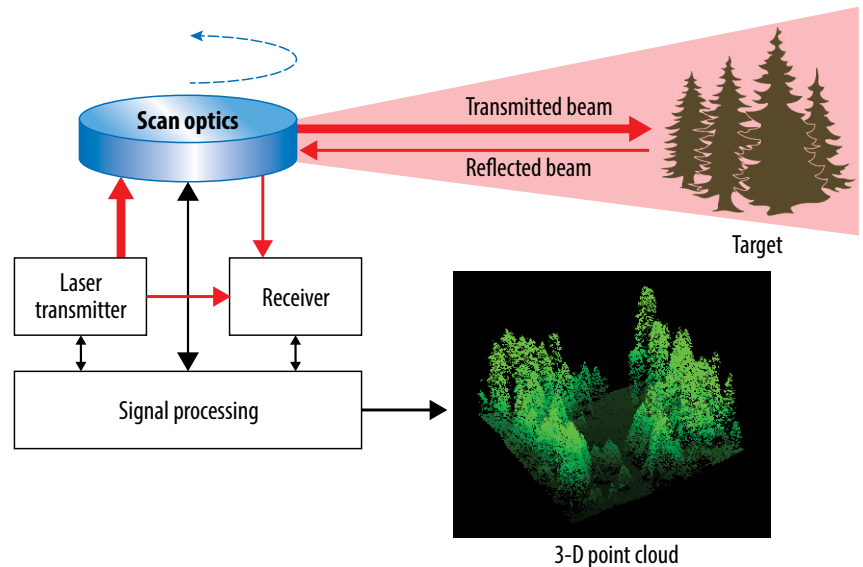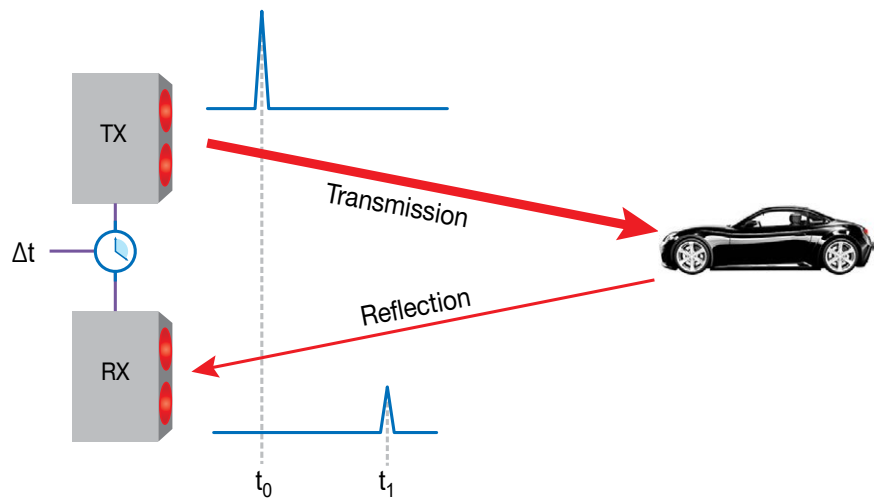

Figure 1. Basic lidar system

Figure 2. Simplified operation of DToF lidar system

4.1 Diode lasers

DToF lidar most commonly uses near-infrared (NIR) semi-conductor laser diodes, either edge-emitting lasers (EELs) or vertical cavity surface emitting lasers (VCSELs). Some typical laser diodes are shown in Figure 3 [9], [10], [11], [12]. Electrically, the laser diode behaves as a very fast PN junction diode. When forward biased above the lasing threshold current, it emits laser radiation with the output optical power approximately proportional to the forward current. Thus, if we drive it with a pulse of current, we get a pulse of laser light [13]. The majority of these lasers have wavelengths in the range of 900 nm to 950 nm, with some choosing 1450 nm to 1550 nm. Other light sources such as fiber lasers may also be used, but diode lasers have a very compelling combination of price, performance, size, reliability, and ease of use.

Diode laser technology has been advancing rapidly in the last decade. For high-power laser diodes, the most obvious advances have been multijunction and parallel lasers on a single die along with a move towards surface mount packages. These techniques allow an increase in the optical power of a given die. Each approach has advantages and drawbacks, and modern high power laser diodes often use both approaches on a single die. Table 1 shows a summary of parameters for a selection of commercially available laser diodes targeted at ToF lidar applications. This is not an exhaustive selection, and it is chosen based on the availability of manufacturers' data rather than actual usage. There are many more lasers available, both packaged and unpackaged, and the number continues to grow.

(a)   (b)

(c)   (d)

Figure 3. Some typical laser diodes used in ToF lidar systems. All diodes are from ams OSRAM: (a) SPL PL90_3, single channel triple junction EEL, (b) SPL S1L90A_3 A01 single channel triple junction EEL, (c) SPL S4L90A_3 A01 quad channel triple junction EEL, and (d) EGA2000-940-W single channel triple junction VCSEL array with diffuser removed.

For laser diodes targeted at pulsed operation, the actual laser die is quite small, especially for EELs. The high power dissipation during the pulse means that the average output power is usually limited to a few watts or less due to thermal management challenges. This means the operating duty cycle for these laser diodes is usually limited to duty cycles of 1% or even as low as 0.1%.

An unfortunate consequence of the optical heritage of laser diodes is that circuit simulation models or the electrical parameters needed to develop such models are often difficult or impossible to obtain from the manufacturer, and this presents a challenge for electrical design. It is hoped that the situation will improve.
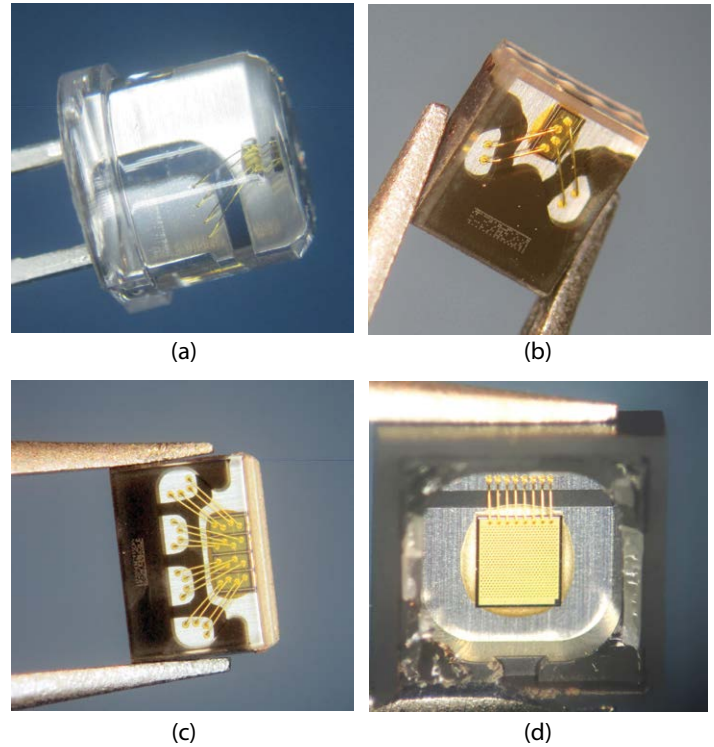
Part Number	Manufacturer	λ [nm]	I_{Fmax} (A)	V_{Fmax} (V)	$P_{opt,max}$ (W)	Technology	Die area [mm²]	Package	L (nH)
SPL PL90_3	OSRAM	905	30	9	75	EEL	Unknown	Through hole	> 5
TPGAD1S09H	Excelitas	905	30	12.5	75	EEL	Unknown	Surface mount	1.6
SPL S1L90A_3 A01	OSRAM	915	40	11	120	EEL	0.24	Surface mount	< 0.5
SPL S4L90A_3 A01	OSRAM	915	160	11	480	EEL	Unknown	Surface mount	< 0.5
EGA2000-940-W	OSRAM	940	10	3.3	7.5	VCSEL	Unknown	Surface mount	< 0.5
TPG3AD1S09	Excelitas	905	40	11.6	120	EEL	Unknown	Surface mount	1.6
RLD90QZW8	Rohm	905	38	13	120	EEL	Unknown	Through hole	> 5
TPGAD1S11A-4A	Excelitas	905	120	12.5	300	EEL	Unknown	Surface mount	< 1
PVGR4S12H	Excelitas	1550	40	100	80	EEL	Unknown	Through hole	5.6
M53-100	Lumentum	905	98	16	400	VCSEL	1.08	Chip	< 0.5

Table 1. A selection of lasers targeted at DToF pulsed lidar applications.

4.2 Pulse requirements

The pulse width of the transmitted optical signal has a great influence on the distance resolution of a lidar system. Figure 4 helps show why this is the case. If we look at the top case, we send narrow pulses of light out from the lidar. Since the light pulse must travel to the target, be reflected, and travel back, for a target at distance d, the time td between pulse transmission and reception is

$$t_d = 2d/c \qquad (2)$$

where c is the speed of light in air, approximately 30 cm/ns (about 1 foot/ns for the imperialists among us). By measuring the time td, we can compute the distance. Now suppose that we send longer duration pulses, as shown in the bottom case. We see that if the pulse length becomes long enough, the reflected pulses begin to overlap, and it becomes harder to distinguish between reflections that represent features in the environment.

For an idea of what pulse lengths are desirable in practice, consider an electrical current pulse width of 1 ns driving the laser diode, which corresponds to an optical pulse length of 30 cm. As features of the target approach 15 cm, the received pulses begin to overlap and become harder to distinguish. While various signal processing techniques can improve the resolution for a given pulse width, it is clear that a shorter pulse gives better inherent precision, and that pulses on the order of a few nanoseconds or less are desirable for human-scale resolution.

Pulse energy determines the range of the lidar. As demand for better resolution drives designs towards narrower pulses, the diode current must increase in order to maintain sufficient pulse energy. Typical pulse current can range from a few amps to hundreds of amps.

Figure 5 provides some typical numbers necessary to drive laser diodes in present-day DToF lidar laser transmitters. They are grouped into long-range and short-range lidars. Note that longer pulse widths are more acceptable for longer range lidar as the distance measurement resolution needs are normally less for distant targets. Commercial lidar is a rapidly changing technology, hence both the numbers and definitions of quantities such as range are still in flux. Nevertheless, these numbers provide an understanding of the parameter space for a DToF laser driver design.
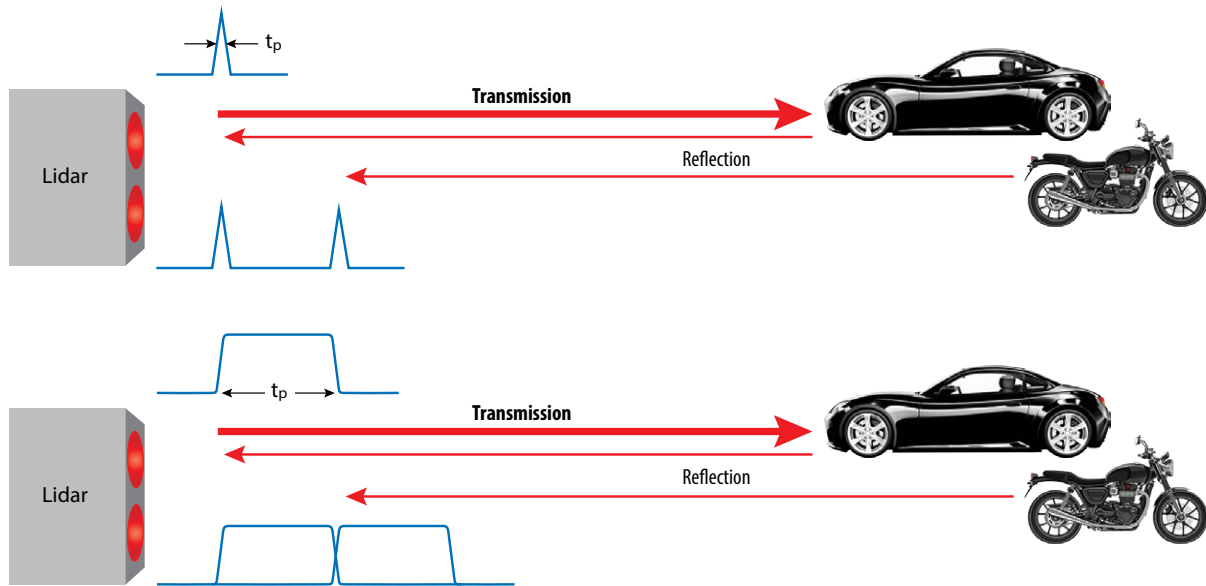

Figure 4. Effect of lidar pulse width on resolution. Top: narrow pulses allow reflections to be easily distinguished. Bottom: wider pulses can overlap, making them harder to distinguish and reducing distance resolution.
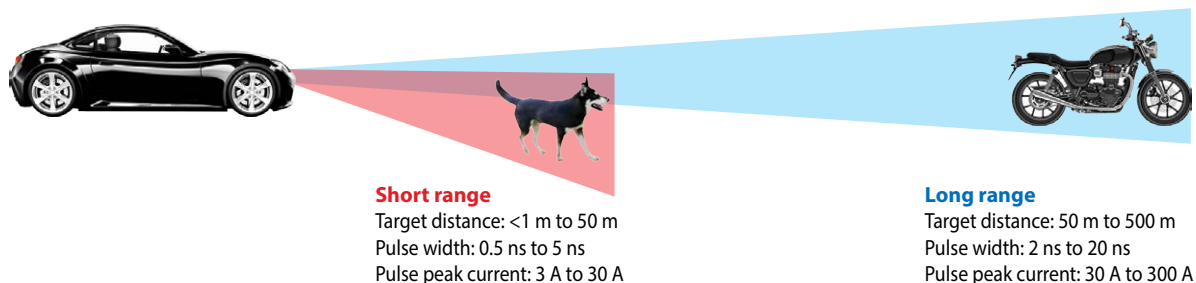

Short range
Target distance: <1 m to 50 m
Pulse width: 0.5 ns to 5 ns
Pulse peak current: 3 A to 30 A

Long range
Target distance: 50 m to 500 m
Pulse width: 2 ns to 20 ns
Pulse peak current: 30 A to 300 A

Figure 5. Typical laser driver specifications for DToF lidar systems

5 Laser drivers

One can find a huge variety of different types of diode laser driver circuits and implementations. This is a result of the vast number of different uses of diode lasers in fields ranging from communication, medicine, law enforcement, material processing, and of course, lidar. The majority of these are functionally equivalent to the circuit shown in Figure 6. This is essentially a common source amplifier. Many laser drivers operate in the linear mode, e.g. the laser current i_{DL} is approximately proportional to the input $v_{command}$. Because this is basically a Class A amplifier, it has the associated low efficiency and hence is not suitable for high power operation due to the high power dissipation in Q_1. Hence, for high power, Q_1 is operated as a switch. This greatly reduces the power dissipation, but the current i_{DL} is now controlled by the bus voltage V_{IN}, the diode semiconductor forward voltage V_{DLF}, and the power loop impedance Z_{PL}. The latter includes the source impedance, $R_{DS(on)}$ of Q_1, and any other parasitic impedance in the circuit. Since Q_1 is operated as a switch, it is a good assumption that any voltage drop due to $R_{DS(on)}$ is small. The impedance Z_{PL} is thus the dominant impedance in the loop. Since it depends on the physical construction of all the components and associated interconnections, it is considered approximately constant and power is thus controlled by varying V_{IN}.

Figure 7 shows a very simple laser driver with all key components visible. There is a high frequency loop denoted as the power loop which consists of capacitor C_1, a stray inductance L_1, a diode laser D_1, and a switch Q_1. There is also a low frequency loop called the charging loop consisting of V_{IN}, Z_{IN}, and C_1. Q_1 is turned on and off by a gate driver GD_1, which is in turn controlled by an input signal $v_{command}$. In normal operation, Q_1 is commanded to turn on and off periodically. The energy needed for transitions in the power loop containing the laser is supplied from C_1, and this energy is replenished via the charging loop. Performance is limited by stray inductance and the speed of the semiconductor power switch.

If we assume for the moment that the switch is ideal, the dominant parasitic component is inductance. Those experienced in power electronics will recognize that this inductance will limit the current risetime, and if the switch is turned off, interrupting a non-zero inductor current is likely cause ringing and its associated problems of voltage stress and EMI generation. If the inductor current is relatively small and the turn-off transition time of Q_1 is relatively slow, the ringing and associated problems are also correspondingly small and thus are tolerable. However, lidar demands extreme currents and fast transitions, which can lead to extreme ringing, overvoltage and EMI. The resonant pulse driver described in the next section is a practical solution to these problems.

5.1 Resonant capacitive discharge laser driver design

There are many kinds of laser driver topologies, but for high power, short pulses, only the resonant design is practical due to the fact parasitic inductance dominates the behavior. Figure 7 shows the simplified schematic of a resonant capacitive discharge laser driver, and Figure 8 shows the main waveforms.
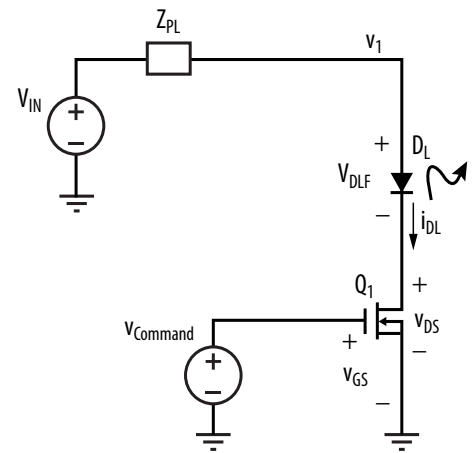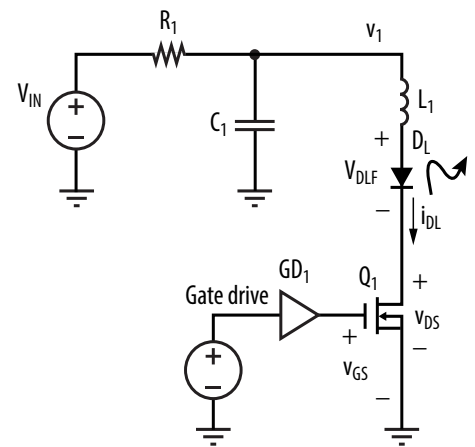

Figure 6. Simple laser driver

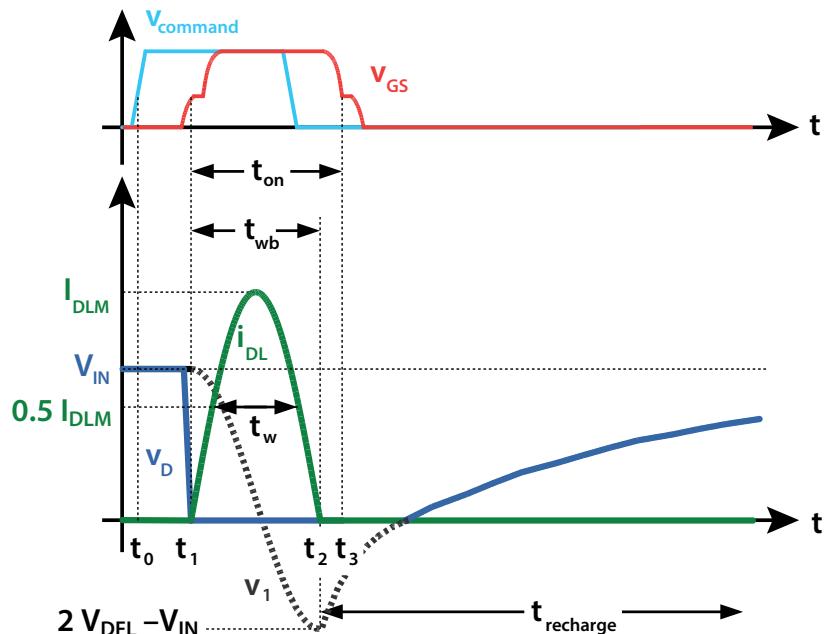*Figure 7. Simple laser driver with parasitic inductance and non-zero power supply impedance*

Figure 8. Key waveforms for capacitive discharge resonant driver of Figure 7

Assuming that Q_1 is an ideal switch, R_1 is large, and D_L is an ideal diode with a fixed forward voltage drop V_{DLF}, the driver works as follows: Q_1 starts in the off-state, so $i_{DL} = 0$. The capacitor voltage $v_1 = V_{IN}$, has been fully charged through R_1. At $t = t_0$, $v_{command}$ triggers the gate drive, turning Q_1 fully on at $t = t_1$. This discharges C_1 through the laser D_L and inductor L_1. C_1 and L_1 form a resonant network, hence i_{DL} and v_{C1} ring sinusoidally. The effective initial capacitor voltage driving the resonance is $V_{C1,0} = V_{IN} - V_{DLF}$ due to the laser diode forward drop. At $t = t_2$, i_{DL} returns to zero and $v_{C1} = 2V_{DLF} - V_{IN}$. At this point D_L prevents the current from reversing and C_1 recharges via R_1. Switch Q_1 is turned off before v_1 crosses zero at $t = t_3$.

The capacitor charging time constant τ_{chrg} and the resonant period t_{res} are

$$\tau_{chrg} = R_1 C_1 \qquad (3)$$

$$t_{res} = 2\pi\sqrt{(L_1 C_1)} = 2t_{wb} \qquad (4)$$

Typically, $\tau_{chrg} \gg t_{res}$, so R_1 has little effect on the L_1–C_1 resonance. The resonant characteristic impedance R_0 and the full width half maximum (FWHM) pulse width t_w are

$$R_0 = \sqrt{\frac{L_1}{C_1}} \qquad (5)$$

$$t_w = t_{res}\frac{\pi - 2\sin^{-1}\frac{1}{2}}{2\pi} = \frac{t_{res}}{3} \qquad (6)$$

This laser driver topology has the following benefits

- The topology utilizes stray inductance
- The pulse shape is stable
- Pulse energy is set via the value of V_{IN}
- Only gate turn-on needs precise control (single edge control)
- Laser current pulse width can be shorter than gate drive minimum pulse width

5.2 Effect of stray inductance

The inductance has a large effect on the design, which we can understand by calculating the peak laser diode current I_{DLpk} using the following equation:

$$I_{DLpk} = \frac{V_{IN} - V_{DLF}}{R_0} \qquad (7)$$

From (4), (5), (6), and (7), we solve for V_{IN} to find

$$V_{IN} = \frac{2\pi L_1}{3t_w}I_{DLpk} + V_{DLF} \qquad (8)$$

Equation 8 allows calculation of the effect of pulse width t_w and peak current I_{DLpk} on the required voltage V_{IN}. Figure 9 illustrates this more clearly. A laser diode voltage drop of $V_{DLF} = 12$ V is assumed, typical of a three or 4 junction laser at operating current. Figure 9a shows the calculated voltage V_{IN} from (7) versus L_1 for a fixed 50 A pulse at several typical values of pulse width, and Figure 9b shows the same for a fixed 2 ns pulse width at various typical values of peak current. It is clearly seen that the required V_{IN} increases approximately linearly with L_1 for a given laser and pulse shape.

5.3 Driver switch properties

The analysis above assumes an ideal switch, but practical semiconductor switches have non-zero switching times and saturation current limits. In addition, switches and their packages can have significant inductance which not only increases the required voltage for a given pulse shape, but also slows switch turn-on.

In the last decade, new power FETs based on GaN have become commercially available. GaN FETs have several overwhelming advantages for lidar applications compared to silicon MOSFETS. First, they have up to 10x lower input capacitance C_{ISS} than MOSFETs of comparable current rating , enabling the GaN FETs to turn on much faster. Second, GaN FETs are a lateral device, which allows the use of a wafer level chip scale package (WLCSP). The WLCSP provides extremely low inductance, excellent thermal performance, high reliability, and minimal cost. Finally, GaN FET die are much smaller than packaged silicon power MOSFETs of comparable voltage and current rating, further reducing inductance, and allowing tight spacing of adjacent lasers for applications such as multi-channel lidar.
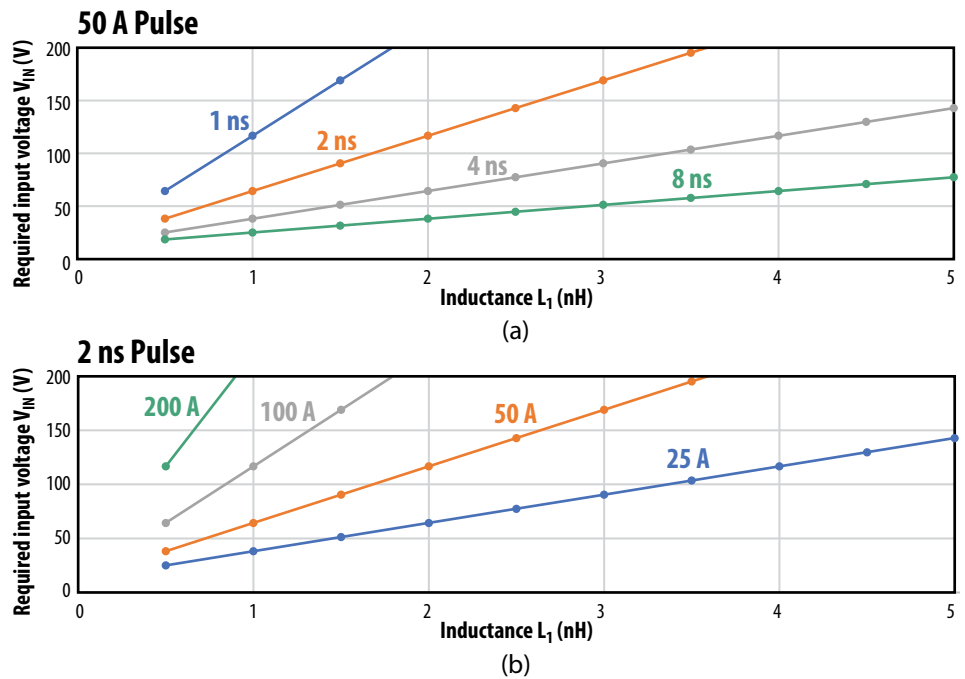

(a)

(b)

Figure 9. Bus voltage V_{IN} versus inductance L_1. (a) shows effect of pulse width for a specific peak pulse current of 50 A, and (b) shows the effect of current for a specific pulse width of 2 ns FWHM.

At the beginning of the twenty-first century, the switch technology of choice was a silicon power MOSFET. Packaging and PCB technology had advanced to where inductance could be controlled sufficiently that values of < 10 nH became feasible. Combined with state-of-the-art silicon MOSFETs, pulse widths of tens of nanoseconds and tens of amps became commercially viable. However, as lidar system designers strive to get more performance, silicon power MOSFETs have become the major limiting factor for two reasons. The first is the large gate charge, which greatly slows the turn-on of the MOSFET. Second, large silicon MOSFETs are vertical devices with connections on both sides of the die. This leads to the use of an external package, which adds substantial inductance in both the power loop and the gate drive loop . The former results in a higher voltage requirement and an even larger die, and the latter further slows the device turn on. As we have seen, this at least a factor of ten worse than the needs of modern lidar systems. Even though ToF lidar had existed for decades, it was relegated to niche applications.

This all changed with the advent of cost-effective gallium nitride (GaN) power FETs. These became commercially available around 2010, with significantly lower inductance and switching figures of merit (FOMs) up to 10x better than comparable silicon MOSFETs. Figure 10 shows three 80 V AEC-Q101 automotive qualified eGaN® FETs, the EPC2252, EPC2204A, and the EPC2218A, with pulse current ratings 75 A, 125 A, and 231 A, respectively [14], [15], [16].

Table 2 shows a comparison of a GaN FET [14] and a state-of-the-art silicon MOSFET [17]. They are selected to have comparable voltage ratings and pulse current ratings and to have automotive qualification, which are key specifications for lidar. It is clear that GaN has large performance benefits over silicon

across the board, and the Gate FOM alone is enough to make the MOSFET unsuitable for high performance DToF lidar. The greatly improved performance of eGaN FETs over the older silicon MOSFET technology translates to much faster switching for a given peak current capability.

Parameter	EPC2252	IAUZ40N08S5N100	Benefit of GaN over Si	Effect on optical pulse
Technology	GaN transistor	Si MOSFET		
Voltage rating $V_{DS,max}$ [V]	80	80	1	Speed, Power
Gate voltage V_{GS} [V]	5	6*	1.2	Speed
Max pulse current $I_{pulse,max}$ [A]	100 (min)	90 (typ)	1.1	Power
Gate FOM $R_G \cdot Q_{Gtot}$ [$\Omega \cdot$ nC]	2.1	15	7.1	Speed
Gate inductance L_G [nH]	<0.2	2.0	>10	Speed, Power
Source inductance L_S [nH]	<0.05	0.25	>5	Speed, Power
Drain inductance L_D [nH]	<0.1	0.1	>1	Speed, Power
Package footprint [mm x mm]	LGA 1.5 x 1.5	DFN 3.3x3.3	6.2	Speed, Power

Table 2. Comparison of GaN FET and silicon MOSFET parameters for devices with comparable pulse current and voltage ratings at 25°C.
*Typical ultrafast gate drives for lidar have 6 V absolute maximum voltage rating.

5.4 Basic design process

Now we can put the above information together in order to design a resonant lidar driver. We start with some specifications on the laser pulse, which will generally result from the system design. These requirements are:

- Pulse peak amplitude I_{DLpk}
- Full width half maximum (FWHM) pulse width t_w
- Pulse repetition frequency PRF
- Laser diode voltage drop V_{DLF}

Once the basic pulse requirements have been chosen, the next factor needed to complete the design is the power loop inductance L_1. The determination of L_1 is discussed in Section 5.5, but for now, assume we can obtain a value.

The required bus voltage V_{IN} is determined from (8), which together with I_{DLpk} is used to select the appropriate part number for FET Q_1.

To determine the value of resonant capacitor C_1, we use (5) and (7) to get

$$C_1 = L_1 \left(\frac{I_{DLpk}}{V_{IN} - V_{DLF}} \right)^2 \qquad (9)$$

The value of recharge resistor R_1 is determined from (3), so that

$$R_1 = \frac{\tau_{chrg}}{C_1} \qquad (10)$$

Since $\tau_{chrg} \gg t_{res}$, we simply need to pick a large enough value of τ_{chrg}. Because of thermal limitations forcing the pulse duty cycle to be typically less than 1% or so, the value of R_1 does not usually need precise determination. This is discussed further in Section 6.4 for those needing to operate at higher duty cycle values.

Together, (8), (9) and (10) determine the remaining values to complete the design.

EPC2252
1.5 x 1.5 mm
Pulsed I_D @125°C = 80 A

(a)

EPC2204A
2.5 x 1.5 mm
Pulsed I_D @125°C = 134 A

(b)

EPC2218A
3.5 x 1.95 mm
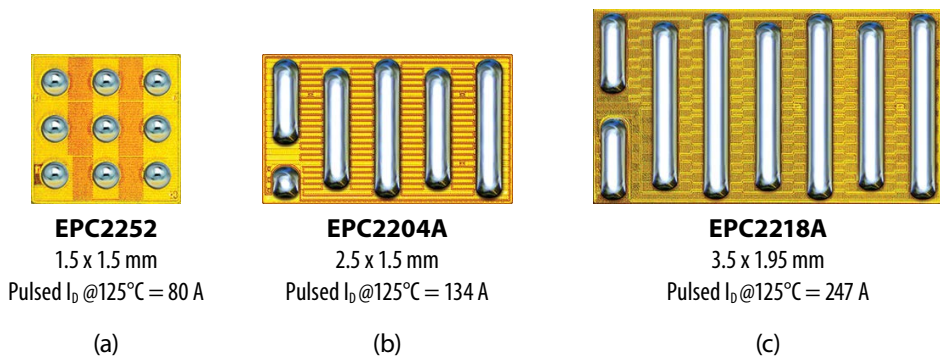Pulsed I_D @125°C = 247 A

(c)

Figure 10. EPC2252 (a), EPC2204A (b), and EPC2218A (c) 80 V eGaN FETs, to scale [12]. Each of these FETs uses a chip-scale package for extremely low inductance and are automotive qualified according to the AEC-Q101 standard.

5.5 Determination of power loop inductance

We have seen that the required input voltage increases nearly linearly with the laser inductance, and the input voltage determines the rating of the FET and the capacitors. Furthermore, the laser driver bus voltage must come from somewhere, most likely another boost converter. The smaller the value of L_1, the simpler and lower cost the rest of the design will be. The core principles of minimizing PCB inductance are explained in depth in [18], which covers a variety of useful techniques for reducing power loop inductance. The referred article shows that with the eGaN FET's chip-scale package, the power loop inductance contribution of the FET, PCB, bus capacitance, and current sensing shunt (if desired) can be kept well below 1 nH and can approach values below 500 pH.

Now, we turn to other sources of inductance, and the main one is the laser. Figure 11 shows typical power loop inductance with a short circuit load and both surface mount and through-hole lasers, as determined by the author's experience. These are superimposed on the graph of Figure 9a to provide an idea of what performance is attainable. A through-hole laser can be expected to lead to a total inductance L_1 of about 5 nH in the absolute best case, but typically it is in the range of 6–20 nH if care is taken to minimize the package lead lengths. Such a high value means that a 50 A pulse of approximately 10 ns is the best that can

be achieved in practice. While a higher voltage part could be used for Q_1, such parts are larger, have greater package inductance, and require greater PCB clearance both between traces on a PCB layer and between layers. All of these factors increase the total inductance further, which results in little improvement being obtained in practice beyond 200 V. Surface mount lasers will result in an inductance L_1 closer to 0.6 nH to 2 nH. In this case, we see that pulses of 2-3 ns are readily achieved with switches rated from 80 V to 100 V.

Note that most of the laser inductance comes from the laser package, including wire bonds. Laser and lidar manufacturers have become aware that the laser package inductance dominate performance, so work is underway to develop advanced packaging or methods of chip scale packaging for laser diodes. This is a greater challenge for high power laser diodes because they have all the constraints of power semiconductors combined with the additional challenge of meeting optical system requirements.

Unfortunately, the value for L_1 is difficult to know exactly at the beginning of the design. This means that it is likely that some iteration will be necessary. For an initial design, consider giving yourself some additional voltage margin, which will allow one to overcome a certain amount of unanticipated inductance.

6 Hardware Driver Design

This section will cover a real laser driver design in some detail by exploring the EPC9179 laser driver development board. The EPC9179 uses an EPC2252, an automotive qualified 80 V eGaN FET with a pulse current rating of 80 A @ 125°C. It is part of a set of development boards (EPC9179, EPC9180, EPC9181) that cover various peak current levels, and these are summarized in Table 3 [7], [19], [20]. All three of these demonstration boards are identical except for the FETs, the resonant capacitors, and the current measurement shunts. All discussion about the operation and physical design is equally applicable to the three boards.

Parameter	Description	EPC9179	EPC9180	EPC9181	Units
Q_1	FET part number	EPC2252	EPC2218A	EPC2204A	n/a
C_{RES} (C2-C6)	Effective total resonant capacitance	1.10	10.8	3.4	nF
I_{peak}	Nominal peak current @125°C for ideal diode load	80	247	134	A
T_{PW}	Nominal pulse width	2-3	5-6	3-4	ns

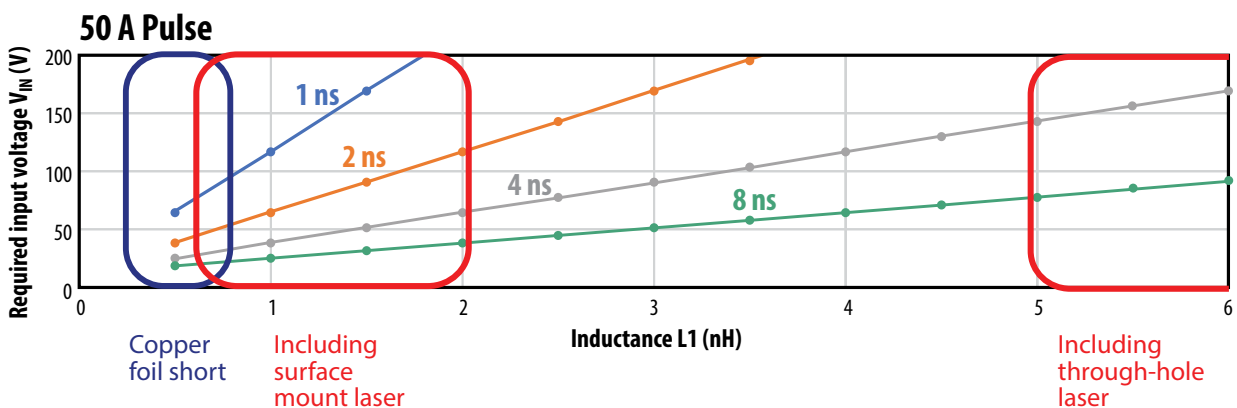*Table 3. EPC Automotive DToF demo boards*

Figure 11. Typical inductance ranges for a well designed laser driver for short circuit load (no laser), surface mount lasers, and through-hole lasers

6.1 Operation

Figure 12 shows the EPC9179 block diagram reproduced from the **EPC9179 Quick Start Guide** (QSG) [7]. The development board supports different types of logic level inputs and include a narrow pulse generator that can produce a fast, short pulse from a longer input pulse (output range approximately 1–50 ns). However, we are only concerned with the main laser driver and test points associated with key waveforms Those interested in greater details can fine this information in both the QSG and the EPC9179 web page [19].

6.2 Construction

The importance of the physical design and construction of a high speed, high current laser driver cannot be overstated. This aspect of design determines the minimum possible inductance. With the use of GaN power switch technology, the switch is no longer the limit and parasitic inductance is the key determining factor of performance. In this section we will cover the key aspects of the physical design, namely the PCB layout.

When considering PCB technology, it is highly desirable to use standard technologies to minimize cost. The designs discussed here use only through-hole vias and a four-layer design. This is enough to illustrate the methods. Some additional performance can be obtained by using blind-, buried-, or micro-vias, but this is not required for basic pulse performance shown here. This is especially true for designs using packaged lasers or lasers with bond wires. Note that use of HDI PCB processes may have other benefits, such as more compact layout and improved thermal performance.

6.2.1 Common source inductance versus power loop inductance

In Figure 7, we added L_1 to model all parasitic inductance in the power loop. This is generally a good approximation for calculating the value of the resonant capacitor, but it obscures one important consideration of high speed, high current switching, namely common source inductance (L_{CS}) [3]. Figure 13 shows L_{CS} as an explicit inductor. The total power loop inductance L_1 is the same, so now we also define L_1 to represent the part explicitly in series with the drain. L_{CS} represent the part of the power loop inductance that is in common with the gate loop, hence the term "common."

Why go through the trouble? Let's consider some typical numbers. Suppose $L_1 = 1$ nH, which would be a well-designed layout with a well-packaged SMT laser diode (see Figure 11). Further suppose that the value of $L_{CS} = 50$ pH. A common rule of thumb is that a bond wire has approximately 1 nH/mm length, so this would be the inductance of a 50 μm bond wire. Finally, the slope of the laser current dI_{ILD}/dt can approach 100 A/ns. In this case, the voltage v_{LCS} across L_{CS} is

$$v_{LCS} = L_{CS} \frac{dI_{LASER}}{dt} = (50 \text{ pH}) \frac{100 \text{ A}}{\text{ns}} = 5 \text{ V} \qquad (11)$$
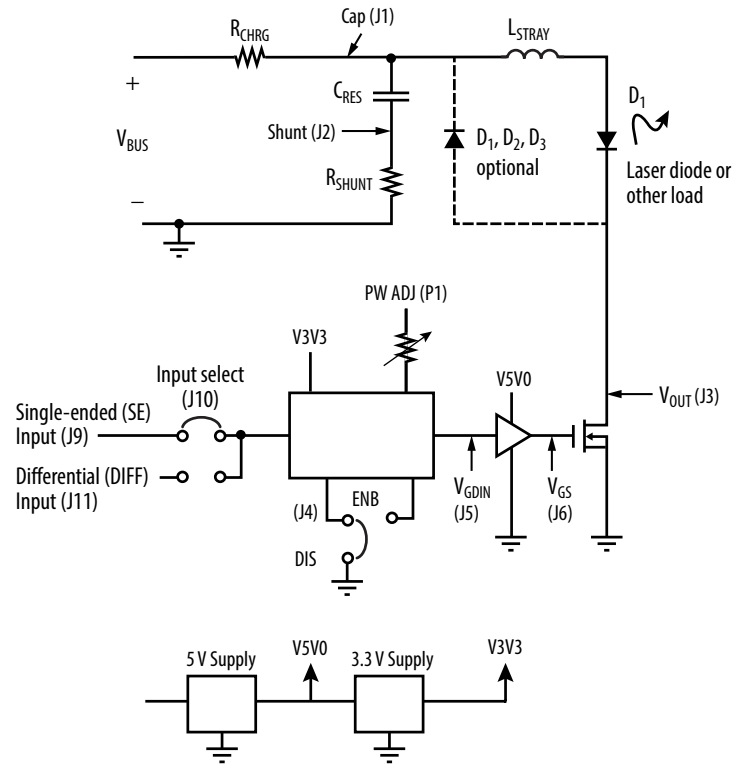

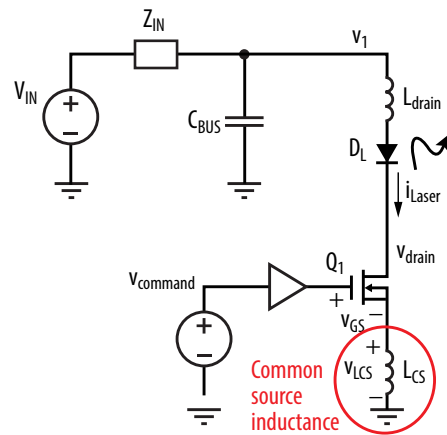*Figure 12. Block diagram of EPC9179, EPC9180, and EPC9181 laser drivers*

Figure 13. Laser driver showing common source inductance L_{CS}

Given that the recommended drive voltage of an eGaN FET is 5 V, and the gate threshold around 2 V, it is clear that 50 pH is unacceptably high. Given that 50 pH can be generated by a 50 um bond wire, we can see how a silicon MOSFET with source bond wires is completely unable to switch fast enough even with an ideal gate drive. It might seem impossible to get a more usable number, say on the order of 10 pH, until we realize that L_{CS} models the coupling of the power loop and gate loop. With this understanding of the role of L_{CS}, we can take a closer look at layout.

6.2.2 Layout

The discussion of layout below requires that the reader is familiar with two key concepts. First, they should be familiar with the principles for minimizing power loop inductance. If they are unfamiliar with the topic or a little rusty, it's worth

reviewing these principles, which can be found here [18]. Second, one must recall that currents will primarily flow in regions of lowest impedance. For high frequency currents or currents that change rapidly, this means they will follow the paths of lowest inductance. Since we are only considering such currents, it is a good assumption that the currents will always travel in the smallest area loop since this has the lowest inductance. Keeping these principles in mind, we now take a look at a high-performance laser driver layout [21].

Figure 14 shows a simplified view of a high-performance laser driver power loop layout, looking at the top of the PCB. First note that the gate drive and power loops are on the left and right sides respectively of the eGaN FET Q_1. Second, note that most of the top layer is a ground plane. Figure 15 shows the flow of current when turning on Q_1. First, referring to Figure 15a, the small arrows on the left shows how the current flows when the gate driver turns the FET on. At this time, the gate driver discharges the gate drive bypass capacitor into the gate of Q_1, as shown by the small red arrow. This same current must flow out of the source back into the other terminal of the bypass capacitor. Since the speed is high, this gate turn-on current will flow in the smallest, lowest inductance path as shown. Once Q_1 is turned on, the power loop current flows. The large red arrows on the right indicate the current discharging from the resonant capacitor C_1. This flows across the top layer into the laser or other load, and then out of the load into the through vias down to the 2nd layer shown in Figure 15b. On the second layer, the power loop current flows left and then up through the vias to the drain of Q_1.

This layout is different from the more usual approach of keeping the second layer an uninterrupted ground or return plane, and there are good reasons behind this. First, each of the gate and power loops have the source current flowing in opposite directions and away from each other, which reduces any common conductive path and also reduces mutual inductance simply due to the increasing physical distance of the two paths. This is made possible due to the interdigitated drain and source terminals as shown in Figure 10. Second, it keeps the power loop source current from flowing through vias. Since vias are a major source of parasitic inductance, this minimizes the source inductance seen by the power loop. The total power loop path would be the same if the current flow were reversed, so the total power loop inductance is unchanged; this layout means that we move some of the power loop inductance from the source to the drain, where it can do little harm.

The PCB layout concepts above allow one to obtain extremely good pulse performance using standard PCB technology. However, pulse performance is only one of several requirements. Thermal performance is often a limiting factor, and in the case of lidar, the laser is part of an optical systems that has its own set of requirements. This layout does have some accommodation for these factors as well. In this layout, the via array connecting the load on the top side to the drain node on the second layer are through vias terminating on a copper land on the bottom of the PCB. This provides a path for heat flow from the load to a heat sink. Since this path is electrically connected to
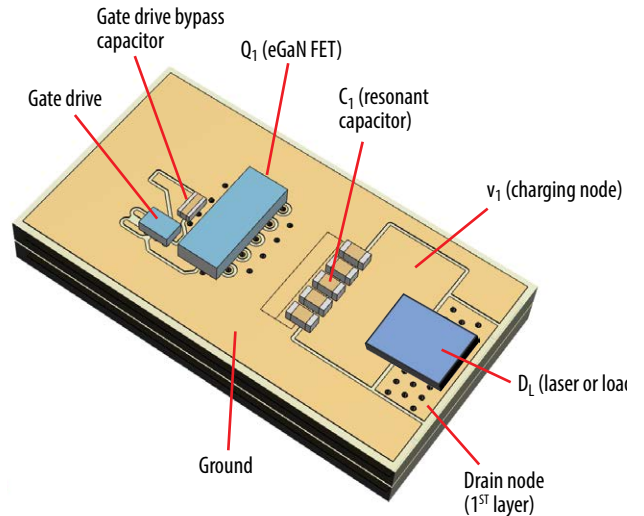

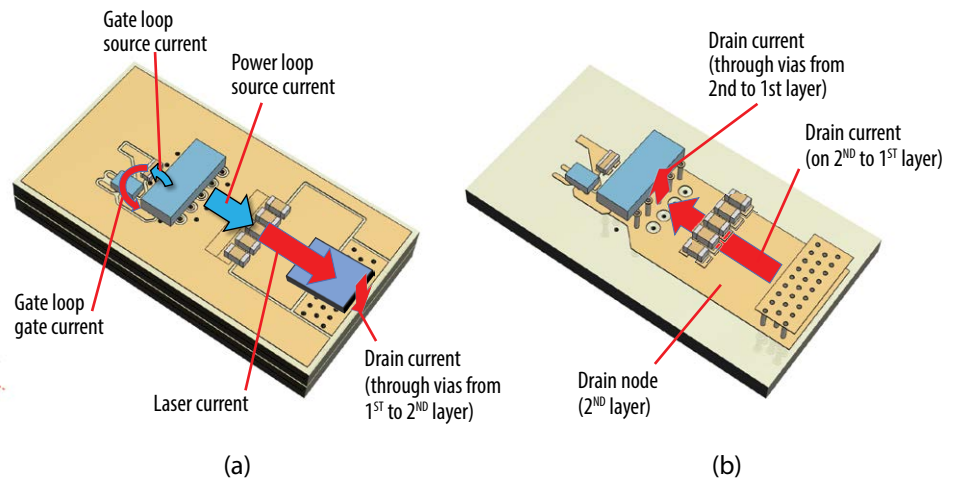*Figure 14. Typical power loop component layout.*

Figure 15. Physical location of power loop currents when FET is turned on

the switch node, the usual methods for heat sinking apply [1]. For optical purposes, the layout shown accommodates EELs by allowing the EEL to be mounted at the edge of the PCB so that the optical output is free and clear of the PCB. The same layout principles are still applicable to VCSELs, but since the latter's optical emission is perpendicular to the PCB plane, the edge mounting is no longer necessary.

Finally, due to the extreme values of dv/dt and di/dt present in the power loop, it is highly recommended to have an additional ground plane underneath the entire power loop structure, and to use via shielding around the entire power loop connecting this plane to the top ground. Clearly there must be gaps in the via shielding to allow connections to the power loop structure, but these should be kept to a minimum. The layout files for the EPC9179/80/81 show examples of a practical implementation.

7 Experimental Results

This section shows experimental results to illustrate the excellent performance that can be obtained by using eGaN FETs and following the design and construction information presented in Section 6.

7.1 Overview of the EPC resonant driver development boards

Figure 16 shows a photograph of the EPC9179 development board, and the expanded view shows the key components of the power loop. Inductance L_1 is not shown because it is strictly due to stray inductance of the power loop components and the PCB, and there is no explicit inductor added in this design. The first three designs (EPC9179, EPC9180, and EPC9181) have nearly identical layouts, and so the inductance of each is similar. The basic design approach is to get the shortest pulse that will be close to the rated current of the device at an operating temperature of 125°C. This is done because in a realistic design, the laser is the main source of heat. Since the laser is mounted in close proximity to the FET, the power dissipation in the laser will result in raising the temperature of the FET. Because the inductance in each case is similar and the voltage ratings are identical, increasing peak current requires increasing the value of the resonant capacitor. This will also cause an increase in pulse width.

The last design (EPC9150) is targeted at high current applications (~200 A) similar to the EPC9180, but where a shorter pulse is desired [22], [23]. Since the layouts have already been optimized for low inductance, and the target currents are similar, Equation (7) shows the only way to decrease the pulse width is to increase the voltage, hence the use of an EPC2034C 200 V FET [24]. It should be noted that the higher voltage design requires other changes, like higher voltage capacitors and increased PCB conductor clearances and interlayer insulation. The two latter factors both act to increase inductances, so one cannot increase voltage indefinitely.

Figure 17 shows the stackups for the two sets of boards, with the dielectric spacing highlighted between the 1st ("Top Layer") and the 2nd ("MidLayer1") layers. The lower voltage
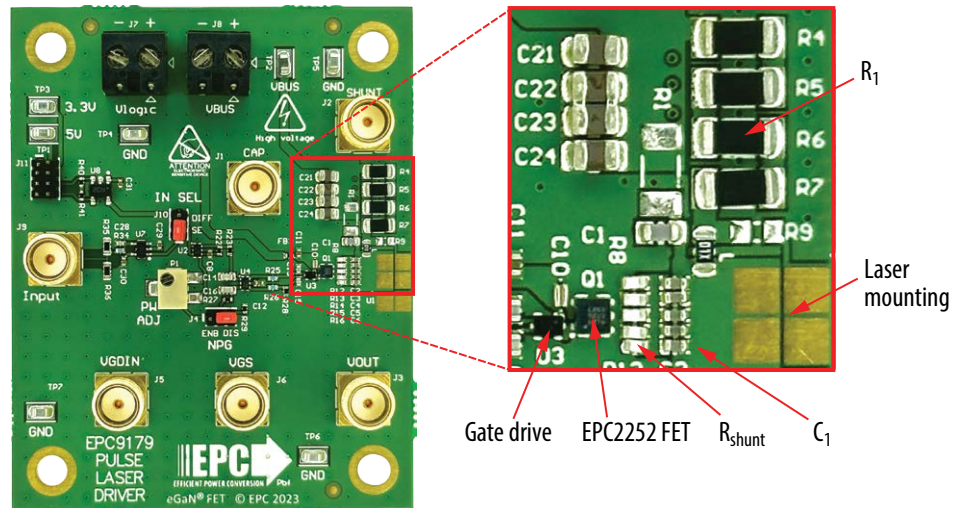

Figure 16. EPC9179 resonant pulse driver with closeup of power loop that highlights the key components of the resonant network. Inductance L_1 is not shown because it is strictly due to stray inductance of the power loop components and the PCB.

Figure 17. PCB stackups used for EPC's development boards. EPC9179, EPC9180, EPC9181 80 V boards (a) and EPC9150 200 V board (b). The thickness of highlighted dielectric layer should be minimized to reduce power loop inductance.

boards are rated at 80 V due to the FETs, but are suitable for 100 V, and use a spacing of 75 μm (3 mils). The higher voltage board is rated at 200 V and uses a spacing of 127 μm (5 mils). These spacings are conservative, and inductance can be reduced by decreasing this spacing. However, since the laser inductance normally dominates the designs in this section, the performance gain may be small.

If better laser packages are available, reducing this thickness may help improve performance. Also, the material used is Isola FR408HR [25]. This is a relatively low-cost material that has better RF properties than standard FR4. This is not strictly necessary from a pulse current performance standpoint, and it was chosen primarily to make the measurement points on the development boards more consistent.

7.2 Experimental waveforms

Selected experimental results are shown for each of the designs in the following subsections.

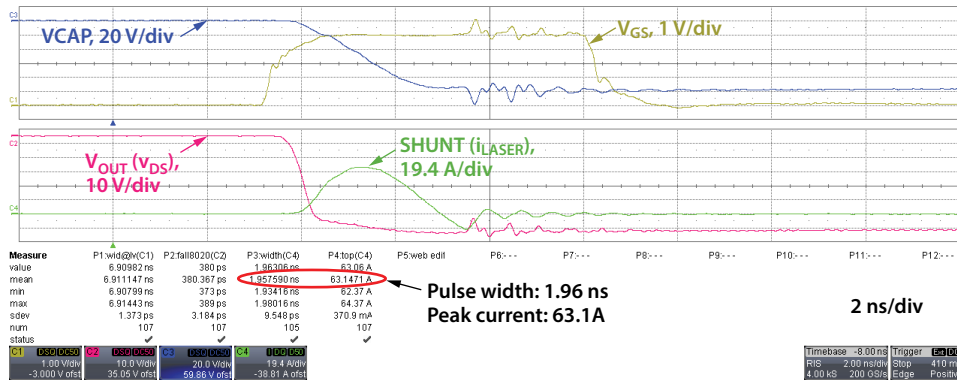### 7.2.1 EPC9179 with EPC2252 Automotive 80 V, 80 A eGaN FET

Figure 18. Waveforms for the EPC9179 demo board using an ams OSRAM SPL S1L90A_3 A01 single channel triple junction laser diode mounted with the EPC9989 interposer. $v_{BUS} = 70$ V.

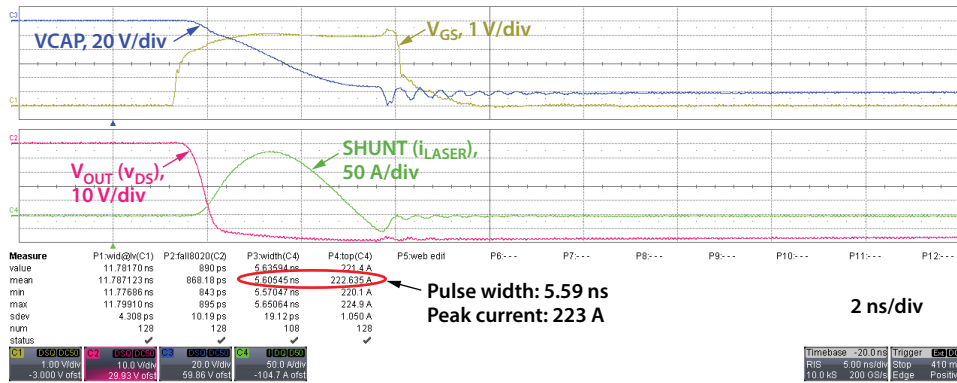### 7.2.2 EPC9180 with EPC2018A Automotive 80 V, 247 A eGaN FET

Figure 19. Waveforms for the EPC9180 demo board using an ams OSRAM SPL S4L90A_3 A01 four channel triple laser diode mounted with the EPC9989 interposer. All channels are connected in parallel. $v_{BUS} = 70$ V.

7.2.3 EPC9181 with EPC2204A Automotive 80 V, 134 A eGaN FET
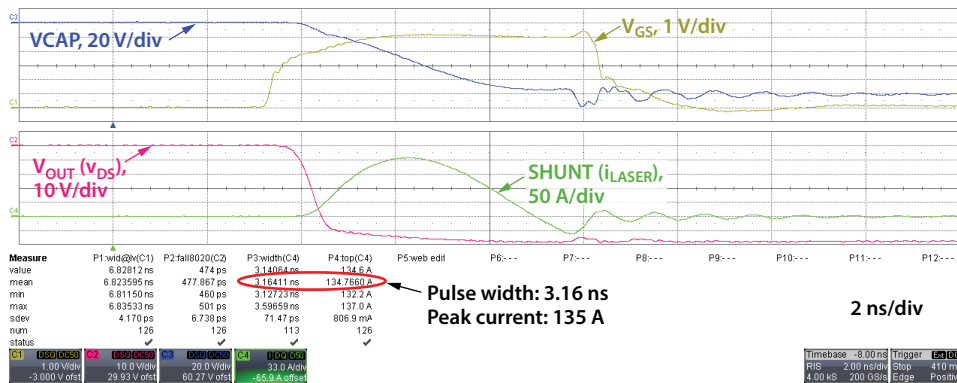

Figure 20. Waveforms for the EPC9181 demo board using an ams OSRAM SPL S4L90A_3 A01 four channel triple laser diode mounted with the EPC9989 interposer. All channels are connected in parallel. $v_{BUS} = 70$ V.
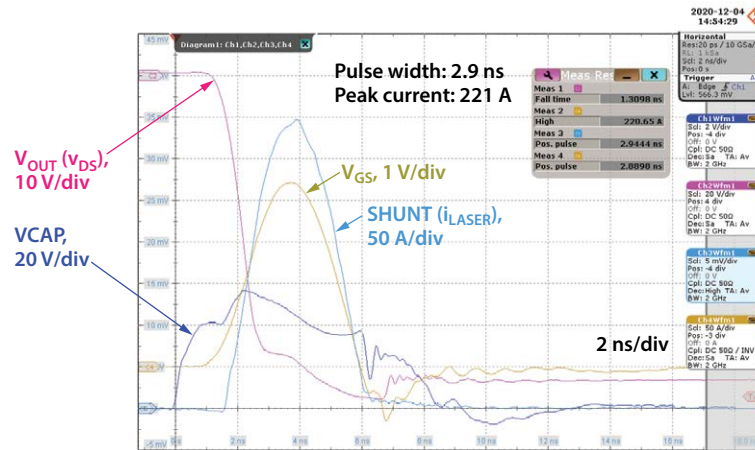
7.2.3 EPC9150 with EPC2034C 200 V, 214 A eGaN FET

Figure 21. Waveforms for the EPC9150 demo board using an ams OSRAM SPL S4L90A_3 A01 four channel triple laser diode mounted with the EPC9989 interposer. All channels are connected in parallel. V_{BUS} = 150 V.

7.3 Summary of Results

Table 4 summarizes the results for the waveforms given above.

Board	FET	Recommended Max Bus Voltage	Laser	Peak current	Pulse width	Peak dId/dt	Peak dVds/dt
EPC9179	EPC2252	70	S1L90A_3 A01	64	2.0	79	132
EPC9180	EPC2218A	70	S4L90A_3 A01	223	5.6	112	60
EPC9181	EPC2204A	70	S4L90A_3 A01	135	3.2	Not measured	Not measured
EPC9150	EPC2034C	160	S4L90A_3 A01	221	2.9	Not measured	Not measured

Table 4. Summary of experimental results for EPC development boards.

8 Additional features of the EPC laser driver development boards

The EPC9179/80/81 series of DToF development boards have a great deal of flexibility and can be used as a base from which to try out new ideas or gain deeper understanding of real component behavior for fast, high current pulses. This section provides some further detail on these designs along with suggestions on different directions to pursue further. The block diagram of Figure 12 applies to the EPC9179/80/81 series and provides a useful reference for this section. While the EPC9150 is an older design, it has most of the features in the newer series, hence most of the discussion in this section is still applicable. If using the EPC9150, please be aware that there are a few differences from the details presented here. The web pages for all the designs include full schematics, PCB

layout files, bills of materials (BOMs), and Quick Start Guides (QSGs) as well as links to related applications notes. These are summarized in the Appendix, and it is recommended to review this material if using the development boards.

8.1 Inputs and outputs

The high speeds involved in laser pulse drivers dictate the use of RF techniques, in particular the use of controlled impedances and the use of a 50 Ω standard impedance for cables and measurements. If you are not sure what this means, there are some good references to get started, as a full explanation is beyond the scope of this article. An excellent reference for those new to the topic is [26].

The input is terminated with a 50 Ω resistance. When connected to a signal source

with a 50 Ω cable, there will be a minimum of ringing and reflection from the input. If using a pulse generator with a 50 Ω output, remember to account for the voltage divider formed by the signal generator output impedance and the input impedance of the board. If it is desired to drive the board with a logic gate directly, please keep in mind that the output impedance of some logic gates can be as high as a few hundred ohms, meaning that they will not drive the input to high enough voltage. In such case, the input terminating resistors can be removed, but the connection to the logic gate must be made in a manner to minimize any ringing or pulse reflections. If this sounds unfamiliar, please review the reference above. There are two possible inputs: a single-ended logic input and an LVDS input [27]. The single-ended input has a logic level translator that is set to be compatible with 2.5 V CMOS

logic levels; this can be changed according to instructions in the QSG. Similarly, the QSG gives instructions on using the LVDS input.

All the outputs are designed to operate properly into a 50 Ω load. This is best accomplished with the use of a 50 Ω coaxial cable connecting to an oscilloscope with a 50 Ω internal input. Please note that the use of external 50 Ω terminators at the scope input is not recommended due to the measurement bandwidth limitation resulting from the high input capacitance of typical 1 megohm scope inputs. This capacitance will usually limit the measurement bandwidth to < 200 MHz, giving a minimum measurement rise time on the order of 2 ns. This too slow for anything beyond verification of basic functionality.

8.2 Voltage sensing with transmission line probes

All sense measurement outputs, except for the shunt measurement, use the transmission line voltage probe principle to obtain waveform fidelity at sub-ns time scales. Such probes typically have a relatively low probing impedance, on the order of 500 to 5k, but the impedance is nearly purely resistive and the bandwidth can be very high, i.e. multiple GHz. These probes are built into the PCB to allow near ideal connection to the node of interest, thus improving waveform fidelity and repeatability. The probe networks and transmission lines are on the bottom of the PCB to minimize interference from the extreme signals in the power loop. They also won't slip off the measurement points, which is an important consideration when measuring the high voltages in the circuit! The basic principles of such probes are discussed in are beyond the scope of this article, but further information can be found in [28].

In order to get useful measurements with the built-in probes, one has to take into account the following three properties. First, they must be connected to an oscilloscope with the scope input set to 50 Ω. The use of a 1 MΩ input with a 50 Ω terminator will severely limit the bandwidth for almost all scopes and is not recommended. Second, each built-in probe has its own attenuation factor that must be considered. These attenuation

factors are given for each board type in its corresponding QSG. Third, the low impedance of the probe means that for points with a large average DC voltage, e.g. drain voltage and resonant capacitor voltage, substantial power dissipation can occur in the probe input resistor. Unfortunately, this resistor must be physically small in order to minimize parasitics, so it will have a very short lifetime due to the resultant heating. To prevent this dissipation, the test points for high voltage measurements include a DC blocking capacitor. This forms a high pass filter that has little effect for the high-speed waveforms of interest. However, if long pulse widths are used, these test points may yield erroneous results, and an external probe should be used. Also, charging and discharging the blocking capacitors will result in extra power dissipation. Finally, the high voltage probes with the blocking capacitors also have a 50 Ω termination on the PCB. This termination prevents leakage currents from charging a connected coaxial cable up to the bus voltage. This is important because if a charged cable is inadvertently connected to the 50 Ω input of a high speed oscilloscope, it can result in an uncomfortable conversation about an expensive oscilloscope repair.

The built-in transmission line probes have been verified to produce near-identical results to a Tektronix P6158 3 GHz transmission line probe [29], so their estimated bandwidth is at least 3 GHz.

8.3 Current sensing

Ahh, current sensing… the bane of power electronics!

There are both pros and cons to current sensing in pulse laser drivers. The pros include verification of operation, timing determination of the laser pulse, control of optical power for maximizing range while meeting eye safety, and troubleshooting. However, current sensing has a long list of cons, including added inductance, increased power dissipation, poor waveform accuracy, cost, reduced drive voltage to overcome inductance, and difficulty of implementation.

Current measurement capability is included in EPC's resonant current pulse drivers in the form of a frequency compensated resistive current shunt. This shunt is in series with the low-potential terminal of the resonant capacitor, as shown in Figure 22. This location allows

the use of a ground-referenced shunt that does not introduce impedance into the source path. As discussed in Section 6.2.1, such source path impedance can be hugely detrimental to performance. Since the charging resistor R_1 is much larger than all other circuit impedances, the capacitor current is nearly equal to the laser or load current.
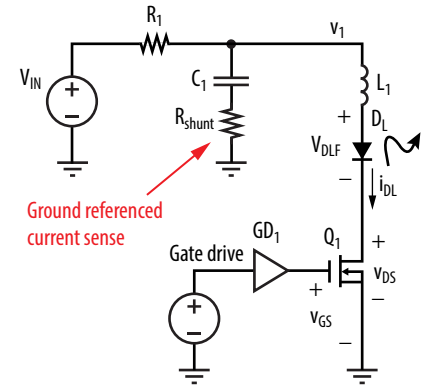

Figure 22. Circuit location of current measurement shunt in resonant pulse development boards.

The need to minimize power loop inductance and the high bandwidth required to measure pulses of a few nanoseconds width means careful attention must be paid to the implementation of the shunt. A typical shunt has parasitic inductance, as shown in Figure 23. There are two parts to this inductance, L_{ESL} and L_{ext}. L_{ESL} is the part of the shunt inductance that contributes to the voltage drop vsense that is used to determine the shunt current, and Lext is an additional inductance to account for the extra distance taken on the PCB as a result of the physical spacing of component pads inter-component spacing. Both inductances should be minimized, but they cannot be eliminated. The sum of L_{ext} and L_{ESL} adds to the power loop, and this must be minimized for maximum performance of the driver. However, its effects on the power loop are straightforward as seen in Section 5. L_{ESL} contributes to the frequency response of the shunt, and its effect is to distort the measurement by adding a zero to the frequency response. Finally, the impedance Z_{sense} of the voltage sensing network provides a path for some of the test current, and this can also contribute to a measurement error.
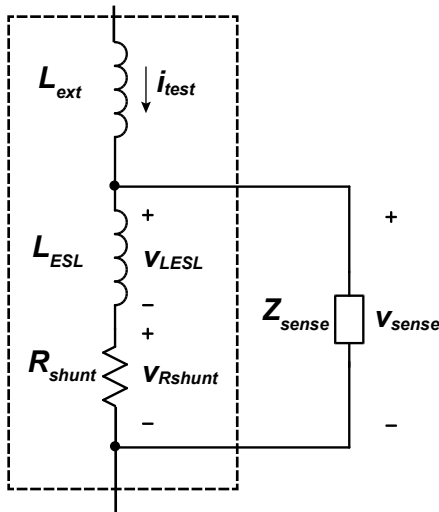
Figure 23. Current measurement shunt resistor with parasitic inductance.

The shunt resistor is comprised of five parallel 0402 resistors integrated as part of the same layout as the rest of the power loop in order to minimize all inductance (Figure 16). To further reduce inductance, the resistors chosen for the design have the resistive element adjacent to the PCB, which reduces the current loop area due to the shunt relative to conventional surface mount resistors. The low duty cycle of DToF laser drivers allows the use of such small resistors even at very high currents.

Normally, it is desired to have a very small resistance value for the shunt to minimize voltage drop due to the high peak current and to minimize the loading effects due to Z_{sense}. Unfortunately, even after the aforementioned steps taken to reduce inductance, enough residual inductance can remain to affect the measurement. The problem is the zero introduced by L_{ESL}, whose location is given by

$$f_{Z,ESL} = \frac{R_{shunt}}{2\pi L_{ESL}} \quad (12)$$

An estimate of the effect can be made by considering the EPC9179. Assuming a rectangular pulse with edge transition times $t_t = 1$ ns gives a 3 dB bandwidth of the pulse of

$$f_{z,shunt} \cong \frac{0.35}{t_t} = 350 \text{ MHz} \quad (13)$$

The partial inductance of the shunt was estimated to be approximately $L_{ESL} = 40$ pH using the results of [21]. From Eqs. 12-13, the inductive reactance for L_{ESL} is

$$|Z_{ESL}| = 2\pi f_{z,shunt} L_{ESL} = 2\pi (350 \text{ MHz})(40 \text{ pH}) = 88 \text{ m}\Omega \quad (14)$$

The resistive value of the shunt should be at least 10x the inductive reactance, which would imply $R_{shunt} \geq 0.88$ Ω. This would result in a voltage drop of 57 V at the peak current of 65 A, which is > 70% of the transistor voltage rating. This would ruin the performance of the design.

The solution to this is to compensate the ESL zero with a pole, which can then allow the use of a much smaller shunt resistor value, in the same manner that a power converter might use inductor equivalent series resistance for current sensing [30]. In practice, it is still best to keep the ESL zero as high as practical without penalizing the overall pulse current performance of the design. The reason is that it is difficult to compensate the ESL zero exactly, so as it is increased in frequency, exact compensation becomes less critical. In the EPC9179, the chosen solution is to pick a value $R_{shunt} = 100$ mΩ, which is selected provide a maximum output voltage of approximately 10% of rated voltage at the max rated current. We can then determine the ESL pole frequency and use an RC network to compensate. If we choose a 50 Ω series resistor for the filter, $R_{shunt} = 100$ mΩ, and $L_{ESL} = 40$ pH, means that a compensation capacitor of 15 pF will create a pole to cancel the zero. Figure 24 shows simulation results for an ideal shunt, an uncompensated shunt, as described, and a compensated shunt using the values given. One can see the error introduced by L_{ESL} and the effectiveness of the compensation. The small glitch at the beginning of the compensated waveform is due to a small 200 pH inductance to check the effect of the capacitor ESL. The width of this glitch is approximately 25 ps which would not be seen in practice due to other bandwidth limitations in the real system (connector, scope, cable, etc.).
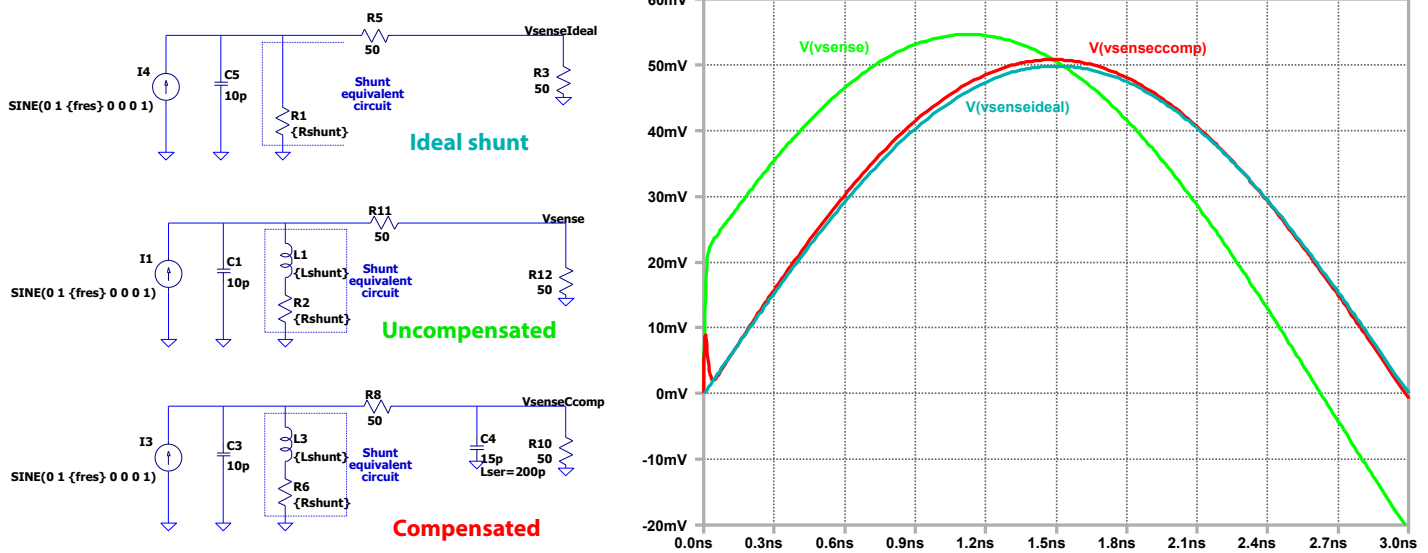

Figure 24. Simulation of current shunts and comparison of results for ideal shunt, uncompensated shunt with ESL, and compensated shunt using RC network. In this simulation, $R_{shunt} = 100$ mΩ and $L_{shunt} = L_{ESL} = 40$ pH. A half-sine pulse with pulse width of 2 ns FWHM.

Determination of the L_{ESL} is not straightforward. In the case of a laser diode load, the shape of the optical waveform can be determined with a high-speed optical detector. The optical power versus current characteristic is usually quite linear above the lasing threshold current of the diode, so the shape of the optical pulse is a good representation of the shape of the current pulse. This method does not provide a good means of determining the absolute pulse amplitude when used with diode lasers, but it can still be used to match the shape of the waveform and its timing relationship with other waveforms. Since the shape is very close to a half-sine, once the compensation yields the correct shape and timing, the result should be fairly accurate. All EPC development boards in this article have been verified with this method, and further work is ongoing to make the procedure more rigorous.

8.4 Resonant capacitors

A parallel set of small surface mount capacitors can be used to make a low inductance capacitor. The example of Figure 16 shows such an implementation using five 0402 capacitors in parallel. Once the inductance has been minimized, the main parameters under the designer's control are voltage and resonant capacitance. Resonant capacitors should use NPO/C0G ceramic dielectric or some other type of dielectric with low loss and linear, stable properties, such as porcelain, glass, or mica. NPO/C0G capacitors are well suited for this application and the cost is low. Fortunately, it has been found when using NPO/C0G capacitors that a set of five parallel 0402 or four parallel capacitors can meet almost all needs up to 200 V. In many cases, the necessary capacitance can be obtained with even fewer capacitors, but there will be some inductance penalty for choosing that route. This is frequently acceptable for many practical lidar designs.

8.5 Resonant capacitor charging

Charging of the resonant capacitor is key to proper operation. There are two main considerations: charging time and charging efficiency. Often, charging time is not a serious concern due to the low duty cycle of

the laser. Until recently, charging efficiency was secondary, but this has changed with the increasing commercialization of lidar systems.

There are two main charging methods: resistive and inductive. Resistive charging is simple to implement and forgiving to the designer, i.e. it has very little impact on the power loop. However, it is not efficient. Inductive charging is usually implemented with a boost or flyback operating in DCM, often using a single pulse charging regime. It has much higher efficiency and the additional advantage of being able to boost a low voltage to the necessary charging voltage. However, the complexity is much higher, and it has the potential to contribute significant parasitics to the power loop. The development boards discussed in this document use resistive charging.

The resonant capacitor is charged through the charging resistor R_1, with a time constant τ_{chrg} given by (3). Since it takes t = 5 τ_{chrg} to charge the resonant cap to > 99% of the final value, we can set the max pulse repetition frequency to PRF = $^1/_5 \cdot \tau_{chrg}$. If a designer wants a higher value of PRF, they can either accept some droop in the laser output, or they can reduce the value of R_1. Reducing R_1 will allow additional current to flow in Q_1 when on, but this is likely to be acceptable for 5 $\tau_{chrg} \gg t_w$.

For an ideal resonant system like that shown in Fig. 5 and the associated waveforms in Fig. 6, we can see that except for the very first time the capacitor C_1 is charged, the initial state of the capacitor is $V_{C1}(t2) = V_{IN} - 2\,V_{DFL}$. It is a good approximation that during recharge, all power dissipation occurs in R_1, and the energy dissipated in R_1 will be

$$E_{R1chrg} = 2C_1(V_{BUS} - V_{DFL})^2 \qquad (15)$$

Note that this is independent of R_1. The power dissipation will be

$$P_{R1chrg} = PRF \cdot E_{R1chrg} \qquad (16)$$

A final consideration with resistive charging as described herein is that if the FET Q_1 is on after the pulse is over, current will flow

through the laser diode, limited by the value of the charging resistor R_1. This will cause some light emission even if the current is below the lasing threshold of the laser diode, known as the LED mode of operation. Although this emission is very small, i.e. 4-5 orders of magnitude below the peak laser emission, the end user should be aware of this and check that it is not a system concern.

8.6 Narrow pulse generator

A narrow pulse generator is also included on the EPC9150/79/80/81 series of boards. This circuit can be used to clean up the input of standard function generators, which by themselves are often not suitable as a signal source because the minimum pulse widths and transition times are often too long. The basic circuit is recommended by the manufacturer of the LMG1020 gate drive used in the boards [31], which is loosely based on the classic Jim Williams design [32]. This circuit can be enabled by a set of jumpers and has an adjustment range of approximately 1 ns to 50 ns, enough to meet most needs.

8.7 Laser mounting

The EPC9150/79/80/81 series of boards was designed for flexibility in the package and mounting of the laser or other load. Figure 16 shows the mounting pads on the PCB. The development boards also ship with the EPC9989 interposer assortment, which is a set of interposers that can be used to mount several commercial lasers as well as an assortment of different pad arrangements to accommodate a wide variety of loads and connectors. The use of an interposer is highly recommended if the laser or other load does not easily fit directly in the PCB, as is provides a repeatable connection with low inductance. The footprint is available online for those who wish to design an interposer for their own purpose [19, 20]. Detailed instructions on the use of the interposers are given in the QSGs for the boards. Figure 25 shows an example of a laser mounted with an interposer.
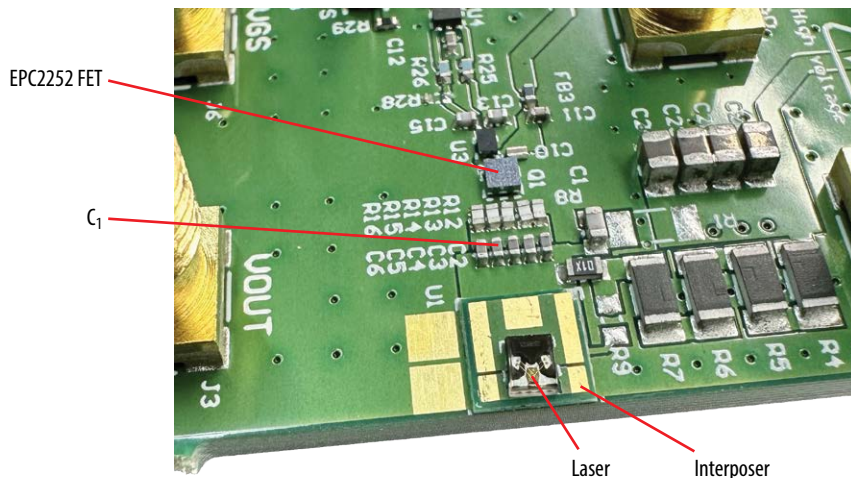
Figure 25. Photograph of an ams OSRAM SPL S1L90A_3 A01 laser mounted to an EPC9179 development board using a low inductance interposer.

8.8 Alternative operating modes and topologies

In most of this article, the discussion has focused on resonant pulse drivers, with many of the advantages discussed in Section 5. However, resonant operation is not the only option. There are two key modifications that the user can make to the main mode of operation, and these are discussed below.

8.8.1 Dual edge control

As discussed, resonant capacitive discharge laser drivers have many useful properties. However, they do have a major limitation, namely that for a given power loop inductance, one has good control over the pulse height, but not the pulse width. Pulse width may also be used to control total pulse energy, and it can be easier to control than pulse amplitude, especially if such control is desired for individual pulses. Furthermore, in some cases, the laser diode or other load will need to be off the PCB. This necessitates some kind of interconnect which will add considerable inductance. Finally, in some cases, there is the need for ultra-fast edges on pulses of arbitrary width. In order to work with some of these limitations, one may use dual edge control, i.e. both turn-on and turn-off of the drive FET are used to control pulse shape.

For typical dual edge control applications, the values of the resonant capacitor and charging resistors will likely need to be changed. Typically, dual-edge control is a move away from resonant operation. Hence, it may be useful to replace the resonant capacitor with a larger value. If so, a change to Class II dielectric capacitors, e.g. X7R, makes sense. In the case where current must be limited, the charging resistor may be used for this purpose, since there is additional bus capacitance at the bus voltage input to the PCB.

Finally, one must consider that the current in the power loop inductance will be interrupted when the switch is turned off, and this is likely to cause ringing and overshoot on the drain terminal of the FET and the laser diode or other load. This ringing will depend on the inductance, the current at the time of turn-off, and the capacitance of the laser, FET, and PCB. There is a provision for the addition of some clamp diodes to control voltage overshoot.

Finding a suitable clamp diode is very challenging. Most diodes have package inductance on the same order or even higher than the power loop inductance, and this limits response speed of the clamp. Furthermore, if the clamp current is high, a diode rated to handle this will tend to have substantial capacitance that will contribute additional ringing, which in some cases can result in repeated output pulses. In lidar applications, the latter is unacceptable. While smaller diodes can work in low duty cycle

applications, and appear to survive, there is little in the way of manufacturers' data about the behavior and reliability under such conditions. Unfortunately, the author cannot recommend a suitable clamp diode at this time. This is an area of open research.

When using the EPC9150/79/80/81 development boards for dual edge control applications, it is recommended that both careful simulation and experimentation are planned. The latter is especially important, as the author's experience is that for diodes selected to have the necessary voltage and current ratings, the available models do not accurately represent the behavior of the diodes for the extremely short transitions found in lidar applications. For commercial applications, a robust program of reliability testing is recommended for the clamp diodes.

The challenges of dual-edge control generally mean that the peak current must be limited to much lower values than discussed in this article. For lidar applications, this is generally the realm of IToF systems. This will be the focus of another article. EPC also makes a series of development boards targeted at IToF applications, and these are listed in the Appendix.

8.8.2 Fail-safe capacitor charging

There is another use case for a clamp diode, which is to provide an alternate charging and discharging path for the resonant capacitor. Such an alternate path is useful in the case where, during a fault that causes the switch Q_1 to stay on, the capacitor charging circuit can provide sufficient current to the laser to cause the system to fail eye safety radiation limits [33], [34]. This can happen at relatively low currents because the laser duty cycle is 100% under such conditions, and the average power can then exceed regulatory limits, which can be prevented using an alternate charging path, as shown in Figure 26.

With the conventional charging scheme, if V_{IN} is high enough and Z_{IN} is low enough, a stuck on command or short circuit failure will result in a continuous current in the laser diode DL. In normal operation, the laser duty cycle is typically 0.1% to 1%, but a small continuous current of a few amps, in some cases < 1 A, can result in higher average power than one would get using 100 A pulses under normal

operation. Using the fail-safe scheme, a short resulting in Q_1 staying on will prevent C_1 from charging and laser D_L from turning on. The EPC9179/80/81 (not the EPC9150) have a provision to employ the fail-safe charging scheme, and the instructions are in the QSG.

The fail-safe scheme has some additional properties of interest. In theory, it will prevent v_{BUS} from going negative and should slow down the turn-off of D_L. In practice, the effect is small. It is supposed that the extra impedance of the diode path slows the diode conduction enough that the turn-off speed penalty is small. However, the effect turns out to be difficult to model and predict at this time, in part due to the fact that the typical diode models do not always reflect behavior accurately at nanosecond time scales, and also because inductive parasitics play a beneficial role here by providing additional impedance that prevents the diode current from increasing so quickly that it affects laser D_L turn-off. This is not yet completely analyzed, but in this case the slow clamping discussed in Section 8.8.1 may be a benefit rather than a drawback. If there are concerns about this, a small resistor in series with D_{clmp} can ensure that the clamp diode path time constant is slow enough to have little effect on D_L turn-off speed. Another benefit of this scheme is that it provides a means for the resonant cap to naturally return to ~ 0 V after the resonant inductor current pulls it below zero. This means that not all the recharging current is supplied from the high potential of v_{BUS} and thus power dissipation in
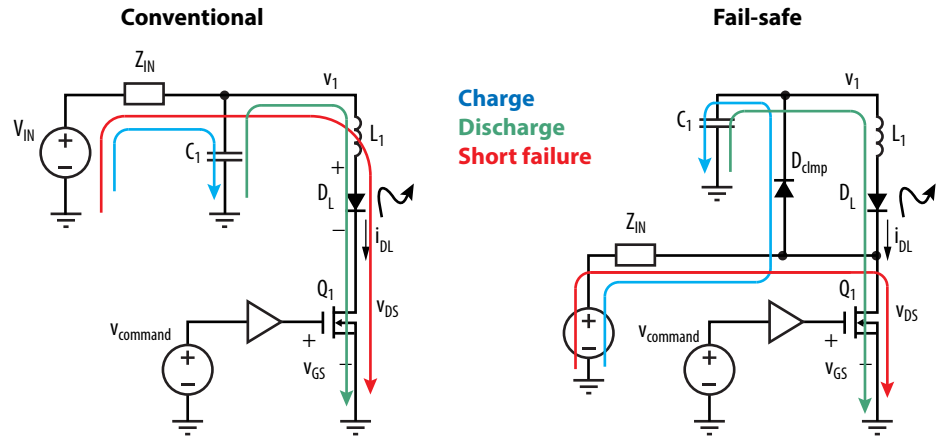

Figure 26. Conventional (left) versus fail-safe (right) charging and discharging paths.

the charging resistor is reduced compared to that given by (15).

Although the fail-safe charging method has some potential advantages, the boards are shipped using the conventional method. This is because the fail-safe charging method is subject to an additional set of parasitic components both within the layout and especially within the diode used for the clamp. This makes operation less predictable and design more ad hoc. However, the method is promising and for a commercial application where the particular laser specifications are set, it is likely that a design can be found. Hence, the option is available in the development board PCB.

9 Conclusion

The superior performance of GaN power transistors and ICs enables the generation of extreme current pulses of tens to hundreds of amps a few nanoseconds wide from a couple square centimeters of PCB area. All this can be done at low cost, in high volume production using standard PCB technology with automotive qualified components. This ability has already revolutionized the lidar market by making affordable, high performance lidar possible in a small form factor. It is likely that there are many other applications for this capability. What can you do with hundreds of amps in a few nanoseconds?
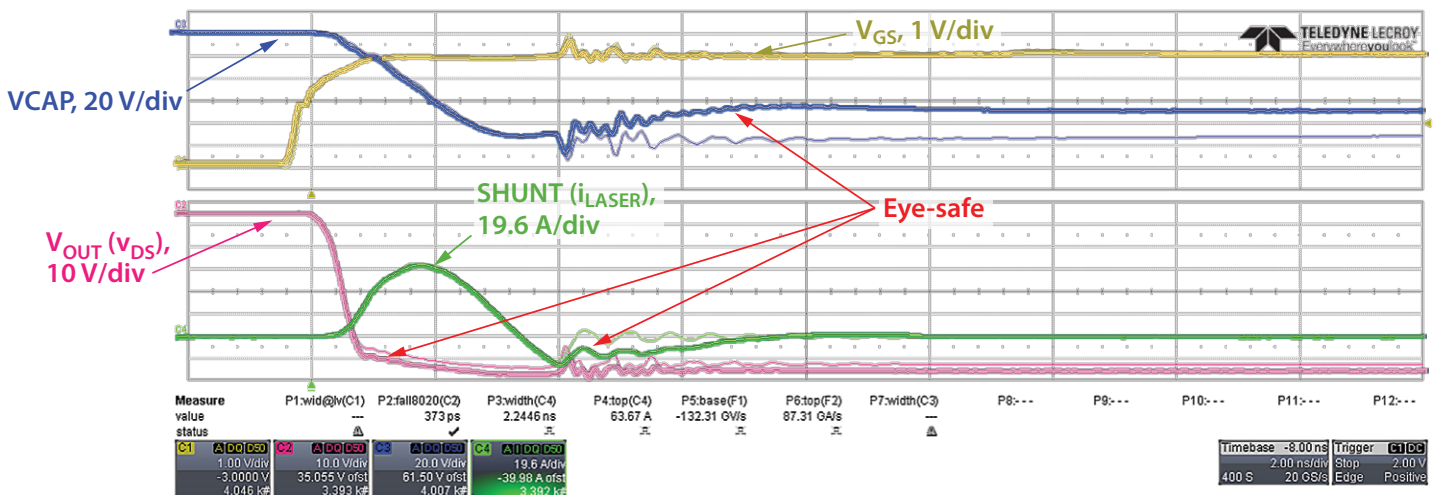

Figure 27. Comparison of conventional and fail-safe charging modes for an EPC9179 evaluation board with an ams OSRAM S1L90A_3 A01 laser installed. The thin traces show the unmodified board and the thick traces show the results with the fail-safe modification.

10 Appendix

Table 5 summarizes a subset of EPC FETs and ICs that have associated development boards targeted for use as laser drivers and other high current pulse applications.

Part Number	Technology	Special Features	Automotive Qualification	Voltage Rating	Pulse Current Rating	Suggested Application	Development Board
EPC2212	eGaN FET		AEC-Q101	100	75	DToF	EPC9126
EPC2001C	eGaN FET		n/a	100	150	DToF	EPC9126HC
EPC2216	eGaN FET		AEC-Q101	15	28	IToF	EPC9144
EPC2034C	eGaN FET		n/a	200	213	DToF	EPC9150
EPC21601	eToF IC	Integrated gate drive with logic level input, 150 MHz	n/a	40	15	IToF	EPC9154
EPC21603	eToF IC	Integrated gate drive with LVDS input, 150 MHz	n/a	40	15	IToF	EPC9156
EPC21701	eToF IC	Integrated gate drive with logic level input, 50 MHz	n/a	80	15	IToF	EPC9172
EPC2252	eGaN FET		AEC-Q101	80	75	DToF	EPC9179
EPC2218A	eGaN FET		AEC-Q101	80	135	DToF	EPC9180
EPC2204A	eGaN FET		AEC-Q101	80	230	DToF	EPC9181
EPC2203	eGaN FET		AEC-Q101	80	17	IToF, DToF	EPC91116

Table 5. Summary of EPC laser and pulse current driver development boards

11 References

[1] A. Lidow, M. de Rooij, J. Glaser, A. Pozo Arribas, S. Zhang, M. Palma, D. Reusch, GaN Transistors for Efficient Power Conversion, 4th ed. Wiley, 2025.

[2] J. Glaser, "How GaN power transistors drive high-performance lidar: Generating ultrafast pulsed power with GaN FETs," IEEE Power Electronics Magazine, vol. 4, no. 1, pp. 25–35, Mar. 2017, doi: 10.1109/MPEL.2016.2643099

[3] Glaser, John S., "GaN-based Solutions for Cost Effective Direct and Indirect Time-of-Flight Lidar Transmitters," presented at the PSMA Power Technology Roadmap Webinar Series, Dec. 10, 2020.

[4] "Global Automotive LIDAR Market Analysis and Forecast Report 2023: A $3.1 Billion Market by 2028 from $555 Million in 2022 - Rising Demand for Autonomous Vehicles/Increasing Sales of Electric Vehicles - ResearchAndMarkets.com," Apr. 07, 2023. Available: https://www.businesswire.com/news/home/20230407005055/en/Global-Automotive-LIDAR-Market-Analysis-and-Forecast-Report-2023-A-3.1-Billion-Market-by-2028-from-555-Million-in-2022---Rising-Demand-for-Autonomous-VehiclesIncreasing-Sales-of-Electric-Vehicles---ResearchAndMarkets.com. [Accessed: Apr. 14, 2024]

[5] P. Boulay, "LIDAR for ADAS and AV Applications: Emerging Trends and Developments," presented at the Automotive LIDAR 2022 Conference and Expo, Online, Sep. 22, 2022. Available: www.automotivelidar.com

[6] Pozo, Alejandro et al., "EPC eGaN® Device Reliability Testing: Phase 12," Efficient Power Conversion Corporation, 2021. Available: https://epc-co.com/epc/Portals/0/epc/documents/product-training/Reliability%20Report%20Phase%2012.pdf

[7] Glaser, John S., "EPC9179, EPC9180, and EPC9181 Quick Start Guide Rev. 2." Efficient Power Conversion Corporation, 2023. Available: https://epc-co.com/epc/documents/guides/EPC9179_qsg.pdf

[8] P. F. McManamon, LiDAR Technologies and Systems. SPIE, 2019. doi: 10.1117/3.2518254. Available: https://www.spiedigitallibrary.org/ebooks/PM/LiDAR-Technologies-and-Systems/eISBN-9781510625402/10.1117/3.2518254. [Accessed: Mar. 02, 2022]

[9] OSRAM Opto Semiconductors, Inc., "SPL PL90_3 Datasheet." Nov. 20, 2015. Available: https://www.osram-os.com/Graphics/XPic3/00194568_0.pdf/SPL%20PL90_3.pdf

[10] ams-OSRAM AG, "SPL S1L90A_3 A01 Datasheet." Jul. 19, 2019. Available: https://ams-osram.com/products/lasers/ir-lasers-eel/osram-smt-laser-spl-s1l90a-3-a01

[11] ams-OSRAM AG, "SPL S4L90A_3 A01 Datasheet." Dec. 20, 2023. Available: https://ams-osram.com/products/lasers/ir-lasers-eel/osram-smt-laser-spl-s4l90a-3-a01

[12]   ams-OSRAM AG, "EGA2000_940_W_Short_Datasheet." Apr. 26, 2021.

[13]   S. Morgott, "Range finding using pulse lasers," Osram Opto Semiconductors, Regensberg, Germany, Application note, Sep. 2004.
Available: http://www.osram-os.com/Graphics/XPic2/00054201_0.pdf/Range%20Finding%20using%20Pulsed%20Laser%20Diodes.pdf

[14]   Efficient Power Conversion Corporation, "EPC2252 data sheet." Jan. 2023.
Available: http://epc-co.com/epc/Portals/0/epc/documents/datasheets/epc2252_datasheet.pdf

[15]   Efficient Power Conversion Corporation, "EPC2204A Datasheet." Aug. 2022.
Available: https://epc-co.com/epc/Portals/0/epc/documents/datasheets/EPC2204A_datasheet.pdf. [Accessed: Oct. 08, 2024]

[16]   Efficient Power Conversion Corporation, "EPC2218A data sheet." May 2023.
Available: http://epc-co.com/epc/Portals/0/epc/documents/datasheets/epc2216_datasheet.pdf

[17]   Infineon Technologies AG, "IAUZ40N08S5N100 data sheet." Sep. 16, 2019.
Available: https://www.infineon.com/dgdl/Infineon-IAUZ40N08S5N100-DataSheet-v01_00-EN.pdf?fileId=5546d4626f1cf1c5016f1e6c94a801de

[18]   D. Reusch and J. Strydom, "Understanding the effect of PCB layout on circuit performance in a high frequency gallium nitride based point of load converter," in 2013 twenty-eighth annual IEEE applied power electronics conference and exposition (APEC), Mar. 2013, pp. 649–655. doi: 10.1109/APEC.2013.6520279

[19]   "EPC9179: 80 V, 75 A Laser Diode Driver Evaluation Board | EPC."
Available: https://epc-co.com/epc/products/evaluation-boards/epc9179. [Accessed: Apr. 14, 2024]

[20]   "EPC9180: 80 V, 230 A Laser Diode Driver Evaluation Board | EPC."
Available: https://epc-co.com/epc/products/evaluation-boards/epc9180. [Accessed: Apr. 14, 2024]

[21]   J. S. Glaser, "Kilowatt Laser Driver with 120 A, sub-10 nanosecond pulses in lt; 3 cm2 using an GaN FET," in PCIM asia 2018; international exhibition and conference for power electronics, intelligent motion, renewable energy and energy management, Jun. 2018, pp. 1–6.

[22]   Efficient Power Conversion Corporation, "Development Board EPC9150 Quick Start Guide," 2021.
Available: https://epc-co.com/epc/Portals/0/epc/documents/guides/EPC9150_qsg.pdf

[23]   "EPC9150: 2000 V, 214 A Laser Diode Driver Evaluation Board | EPC."
Available: https://epc-co.com/epc/products/evaluation-boards/epc9150. [Accessed: Apr. 14, 2024]

[24]   Efficient Power Conversion Corporation, "EPC2034C data sheet." Jun. 2020.
Available: http://epc-co.com/epc/Portals/0/epc/documents/datasheets/epc2034c_datasheet.pdf

[25]   Isola Group, "Isola FR408HR data sheet," Aug. 2017,
Available: http://www.isola-group.com/wp-content/uploads/data-sheets/fr408hr.pdf. [Accessed: Oct. 14, 2017]

[26]   Howard Johnson and Martin Graham, High Speed Digital Design: A Handbook of Black Magic, 1st Edition. Prentice Hall, Inc., 1993.

[27]   "LVDS Application and Data Handbook," 2002.

[28]   J. Weber, "Oscilloscope probe circuits," Tektronix, Inc., 1969.

[29]   Tektronix Inc., "Tektronix P6158 20X 1 kohm Low Capacitance Probe For 50 Ohm Oscilloscopes, 071-0123-00." Feb. 24, 1998.
Available: https://download.tek.com/manual/071012300.pdf

[30]   Linfinity, Inc., "A simple current-sense technique eliminating a sense resistor," Jul. 1998.

[31]   Texas Instruments, "LMG1020 5-V, 7-A, 5-A Low-Side GaN and MOSFET Driver For 1-ns Pulse Width Applications datasheet (Rev. B)." Oct. 16, 2018. Available: https://www.ti.com/lit/gpn/lmg1020

[32]   J. Williams, "Signal sources, conditioners and power circuitry - circuits of the fall, 2004," Linear Technology, Application note AN98, Nov. 2004.

[33]   S. Morgott, "Optical radiation safety information," Osram Opto Semiconductors, Application note, Dec. 2004.
Available: http://www.osram-os.com/Graphics/XPic4/00018294_0.pdf/Optical

[34]   "IEC 60825-1:2014 Safety of laser products - Part 1: Equipment classification and requirements." International Electrotechnical Commission (IEC), May 15, 2014. Available: https://webstore.iec.ch/en/publication/3587